Carbohydrate Polymers 101 (2014) 464–470

Contents lists available at ScienceDirect

Carbohydrate Polymers

journal homepage: www.elsevier.com/locate/carbpol

Evaluation of the effects of chitin nanofibrils on skin function using skin models

Ikuko Ito [a], Tomohiro Osaki [a,*], Shinsuke Ifuku [b], Hiroyuki Saimoto [b], Yoshimori Takamori [c], Seiji Kurozumi [c], Tomohiro Imagawa [a], Kazuo Azuma [a], Takeshi Tsuka [a], Yoshiharu Okamoto [a], Saburo Minami [a]

[a] Department of Veterinary Clinical Medicine, School of Veterinary Medicine, Tottori University, 4-101 Koyama-Minami, Tottori 680-8553, Japan
[b] Graduate School of Engineering, Tottori University, 4-101 Koyama-Minami, Tottori 680-8553, Japan
[c] Koyo Chemical Co., Ltd., Takenouchi Danchi 217, Sakaiminato, Tottori 684-0046, Japan

ARTICLE INFO

Article history:
Received 23 August 2013
Received in revised form
20 September 2013
Accepted 21 September 2013
Available online 1 October 2013

Keywords:
Chitin nanofibrils
Three-dimensional skin culture model
Franz cells
Skin
Skin-protective agents

ABSTRACT

Chitins are highly crystalline structures that are predominantly found in crustacean shells. Alpha-chitin is composed of microfibers, which are made up of nanofibrils that are 2–5 nm in diameter and 30 nm in length and embedded in a protein matrix. Crystalline nanofibrils can also be prepared by acid treatment. We verified the effect of chitin nanofibrils (NF) and nanocrystals (NC) on skin using a three-dimensional skin culture model and Franz cells. The application of NF and NC to skin improved the epithelial granular layer and increased granular density. Furthermore, NF and NC application to the skin resulted in a lower production of TGF-β compared to that of the control group. NF and NC might have protective effects to skin. Therefore, their potential use as components of skin-protective formulations merits consideration.

1. Introduction

Alpha-chitin is composed of microfibers, which are made up of nanofibrils (NF) that are approximately 2–5 nm in diameter and 30 nm in length and embedded in a protein matrix (Chen, Lin, McKittrick, & Meyers, 2008; Fabritius et al., 2012; Nikolov et al., 2011; Raabe et al., 2006). Isolated chitin NF show a potential for use in drug delivery systems, the tissue engineering of scaffolds, and wound dressing (Muzzarelli et al., 2007). Acid hydrolysis is one of the main methods used to prepare chitin NF (Gopalan & Dufresne, 2003; Revol & Marchessault, 1993). Moreover, ultrasonication of squid pen beta-chitin under acidic conditions yields 3–4-nm-wide chitin NF with relatively low crystallinity (Fan, Saito, & Isogai, 2008). Chitin nanofibers are easily prepared using either fine grinding or wet-type atomization methods (Ifuku & Saimoto, 2012).

Chitin and chitosan have an accelerating effect on the wound healing process and regulate immune response (Muzzarelli, 2009, 2010). Recently, Chitin and chitosan could be used as nanofibrils. However, it is unclear whether chitin NF could maintain original function or not.

We have previously found that chitin NF improve the clinical symptoms and suppress the onset of ulcerative colitis in an animal model (Azuma et al., 2012). Furthermore, chitin NF suppressed myeloperoxidase activation in the colon and decreased serum interleukin (IL)-6 concentrations. In contrast, the application of chitin powder did not produce any anti-inflammatory effect (Azuma et al., 2012).

Because many people exhibit skin hypersensitivity in response to cosmetics and textiles, the development of materials exempt from inflammatory activity is essential. In the present study, we describe a novel three-dimensional skin model assay to evaluate the skin-protective effects of chitin NF.

2. Materials and methods

2.1. Preparation of chitin nanofibers and chitin nanocrystals

Chitin nanofibers and nanocrystals were prepared as described previously (Gopalan & Dufresne, 2003; Ifuku et al., 2010). In brief,

* Corresponding author at: Laboratory of Veterinary Surgery, Faculty of Agriculture, Tottori University, Tottori 680-8553, Japan. Tel.: +81 857 31 5434; fax: +81 857 31 5434.
E-mail addresses: i.ikuko95@gmail.com (I. Ito), tosaki@muses.tottori-u.ac.jp (T. Osaki), sifuku@chem.tottori-u.ac.jp (S. Ifuku), saimoto@chem.tottori-u.ac.jp (H. Saimoto), takamori@koyo-chemical.co.jp (Y. Takamori), kurozumi@koyo-chemical.co.jp (S. Kurozumi), imagawat@muses.tottori-u.ac.jp (T. Imagawa), kazuazu85@yahoo.co.jp (K. Azuma), tsuka@muses.tottori-u.ac.jp (T. Tsuka), yokamoto@muses.tottori-u.ac.jp (Y. Okamoto), sabminami@nifty.com (S. Minami).

0144-8617/$ – see front matter © 2013 Elsevier Ltd. All rights reserved.
http://dx.doi.org/10.1016/j.carbpol.2013.09.074

dry chitin powder from crab shell was dispersed in water at 1 wt.%, and acetic acid was added to adjust the pH value to 3 to facilitate fibrillation. The chitin was roughly crushed with a domestic blender. Finally, the slurry was passed through a grinder (MKCA6–3; Masuko Sangyo Co., Ltd.) at 1500 rpm. Chitin crystals were prepared by hydrolyzing the chitin with 3 N HCl at the boil for 90 min under stirring. After acid hydrolysis, the suspension was washed with distilled water by centrifugation thoroughly. The precipitate was dispersed in water at 1 wt.%, and acetic acid was added to adjust the pH value to 3. The chitin was passed through a grinder.

2.2. Test materials

Test using 3D human skin culture model: we prepared a 1% chitin NF dispersion and a 1% chitin nanocrystal (NC) dispersion at pH 3 and pH 6 by the grinding method described by Ifuku and Saimoto (2012). Control solutions were distilled water, or acetic acid at pH 3 and pH 6 (AC); 1% N-acetyl-D-glucosamine (GlcNAc) was used as a positive control for effect of the keratinocyte growth factor (Minami & Okamoto, 2010).

Test using Franz diffusion cells: we prepared samples of 1% chitin nanofibrils and nanocrystals under the following conditions (Ifuku & Saimoto, 2012): pH 6, pH 6 Ac, and DW.

2.3. Test procedures using 3D human skin culture model

The three-dimensional epidermal model LabCyte EPI-MODEL 24 (Tissue Engineering Japan Co., Aichi) was used to test the contact effect of each sample. This model, which includes skin layers between the keratin layer and the basal layer, was incubated at 37 °C in a 5% CO_2 humidified atmosphere.

The 9 conditions tested in this experiment are as follows: (1) no application (NON) ($n = 8$); (2) distilled water (DW) ($n = 12$); (3) 1% acetic acid (AC) solution, pH 3 ($n = 8$); (4) 1% AC solution, pH 6 ($n = 8$); (5) 1% chitin NF dispersed at pH 3 ($n = 8$); (6) 1% chitin NF dispersed at pH 6 ($n = 12$); (7) 1% chitin NC dispersed at pH 3 ($n = 8$); (8) 1% chitin NC dispersed at pH 6 ($n = 12$); and (9) 1% GlcNAc ($n = 12$).

The assay media (0.5 mL/well) (Tissue Engineering Japan Co., Aichi) was aliquoted into the assay plate (Tissue Engineering Japan Co., Aichi). Next, the three-dimensional skin culture model was placed in each well. The assay plates were then incubated in a CO_2 incubator for 1 h. The test material (50 μL/well) was applied to the keratin layer of the three-dimensional skin culture model after the 1-h incubation.

The three-dimensional human skin culture models were removed from the assay plate at 4, 12, and 24 h post-application, and the cultured skin (from the keratin to basal layers) were harvested.

2.4. Histological observations

The harvested skin culture was immersed and fixed in 10% formalin (Mildform 10 N, Wako Pure Chemical Industries Ltd., Osaka, Japan). Cross-sectional slices (4-μm-thick) were soaked in hematoxylin and eosin (H&E) and histological evaluations were conducted. The samples were prepared by Sumika Technoservice Corporation (Osaka, Japan). The H&E stained samples from each experimental group were evaluated using an optical microscope (BX51-FL, Olympus Corporation, Tokyo). The tissue image analysis was done using Lumina Vision (Ver. 2.5.2.1, Mitani Corporation, Tokyo, Japan).

Images for 4 non-continuous fields of view at 400× magnification were taken for each H&E-stained sample in each experimental group. Sample scores were calculated by averaging the observational scores from one quadrant of the image for the granular layer and stratum spinosum. The below criteria were used to convert the observations into a score.

2.5. Assessment of the granular layer and the stratum spinosum

The number of granular layers and the granule cell density of the layers were evaluated.

A complete absence of the granular layer was assigned a score of 0; a partial granular layer was assigned a score of 1; if 1, 2, 3, or 4 layers were present, scores of 2, 3, 4, and 5, respectively, were assigned.

The granule cells lacking keratohyalin granules were assigned a score of 0, a weak presence was assigned a score of 1, a moderate abundance with a high dye-affinity was assigned a score of 2, and a granule cell with abundant granules was assigned a score of 3.

The stratum spinosum quality was evaluated by measuring the width of the intercellular gap and the clarity of the nucleus. A score of 0 was assigned if the intercellular contacts in the stratum spinosum had collapsed; (1) if the intercellular gap was greater than 1 mm at 400× magnification; (2) if the space was less than 1 mm; and (3) if a space could not be confirmed by the naked eye, when I displayed the image which photographed at magnification 400 times with 122 mm in height, size of 163 mm in width In addition, a score of 1 was assigned if the nucleus was clearly visible; otherwise, a score of 2 was assigned.

2.6. Test procedures using Franz diffusion cells

Franz diffusion cells (PermeGear Inc., Keystone Scientific K.K., Japan) were used to evaluate the test model. Skin removed from Hos:HR-1 mice (8–9 week-old, 25–35-g males, Hoshino Laboratory Animals, Inc., Ibaraki, Japan) was used. The use of the animals and the procedures they underwent were approved by the Animal Research Committee of Tottori University.

The 4 experimental conditions were as follows: (1) DW ($n = 4$); (2) 1% AC solutions of pH 6 ($n = 4$); (3) 1% chitin NF dispersed at pH 6 ($n = 4$); and (4) 1% chitin NC dispersed at pH 6 ($n = 4$).

Skin samples removed from mice sacrificed by cervical dislocation were applied to 1× phosphate buffered saline (PBS 10×, pH 7.4; Life Technologies Corporation, Tokyo, Japan)-soaked Franz cells. The cells were incubated in a thermostat chamber for 1 h (TERMO MINDER EX; Taitec Corporation, Saitama, Japan). Each test material was then applied and the cells were re-incubated. A graphical illustration of the methods is shown in Fig. 1.

At 1, 3, and 6 h post-application, PBS was aspirated from the cells. Approximately 1 and 3 h after removal of PBS, fresh PBS was injected into Franz cells using a disposable feeding needle (FG6206; Fuchigami, Kyoto, Japan), and reincubated. The aspirated PBS was concentrated using a centrifuge (SCT 5BA, Hitachi Koki Co., Ltd., Tokyo) at 4000 × g for 20 min at room temperature. The concentrated PBS was stored at −80 °C until analysis.

2.7. Measurement of cytokine concentrations in PBS

We measured the concentration of IL-1α and TGF-β using a commercially available cytokine measurement kit (Mouse, ELISA Kit, Quantikine M (96 well), R&D Systems, Minneapolis, USA). In addition, we calculated the cumulative cytokine production level through the summation of cytokine concentrations at each time point.

2.8. Statistical analysis

Analysis was performed using 4 step Excel Statistics (OMS Publishing, Saitama, Japan). For each investigation, we performed the

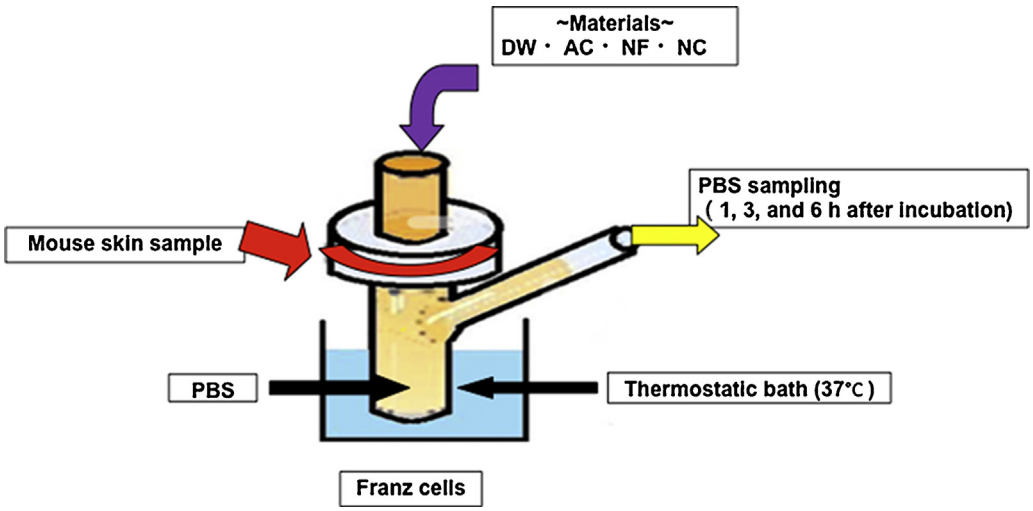

Fig. 1. Schematic of the protocol for Experiment 2. Skin samples were applied to PBS-soaked Franz cells. The samples were incubated in a thermostat chamber for 1 h. Each test material was then applied and the samples were re-incubated. At 1, 3, and 6 h post-application, PBS was aspirated from the cells.

Bartlett test for normality; for those where we confirmed normality or equal variance, single factor ANOVA was performed; otherwise, we used the Kruskal–Wallis test. Afterwards, a multiple comparison test (the Tukey–Kramer test or Scheffe's *F* test) was performed. A risk ratio of less than 5% ($p < 0.05$) was considered significant. A risk ratio less than 1% ($p < 0.01$) was considered highly significant.

3. Results

3.1. Experiment 1: effect of chitin NF on epithelial cells using a three-dimensional skin culture model

Histological observations for each group are shown in Table 1. In the NON group, the granular layer score was 2.5 and granule

Table 1
The results of histological scoring in each group.

		Nucleus clearly	Intercellular gap	Granule density	Number of the granule layers	Total (mean ± SE)
NON	4 h	0.81	0.84	2.19	2.94	6.78 ± 0.51
	12 h	0.34	0.34	2.19	3.13	6.00 ± 0.32
	24 h	0.38	0.25	1.88	3.09	5.59 ± 0.19
DW	4 h	0.71	0.56	1.92	3.08	6.27 ± 0.23
	12 h	0.75	0.63	1.60	2.42	5.40 ± 0.35
	24 h	0.73	0.21	1.15	2.10	4.19 ± 0.38
Ac (pH3)	4 h	1.00	1.44	1.75	2.84	7.03 ± 0.18
	12 h	1.00	1.00	1.34	2.50	5.84 ± 0.34
	24 h	0.94	1.13	1.06	1.75	4.88 ± 0.44
Ac (pH6)	4 h	0.84	1.00	2.16	3.03	7.03 ± 0.21
	12 h	0.69	0.97	1.75	2.63	6.03 ± 0.27
	24 h	0.91	0.66	1.53	2.31	5.41 ± 0.31
NF (pH3)	4 h	0.97	1.84	1.91	2.69	7.41 ± 0.41
	12 h	1.00	1.28	1.34	2.28	5.91 ± 0.30
	24 h	0.97	1.56	0.84	1.75	5.13 ± 0.37
NF (pH6)	4 h	0.92	1.33	2.54	3.63	8.42 ± 0.18
	12 h	0.96	1.06	1.90	2.69	6.60 ± 0.17
	24 h	0.94	1.04	1.73	2.65	6.35 ± 0.30
NC (pH3)	4 h	1.00	1.06	1.81	2.84	6.72 ± 0.30
	12 h	1.00	1.06	1.16	2.00	5.22 ± 0.33
	24 h	0.97	1.00	0.47	1.28	3.72 ± 0.30
NC (pH6)	4 h	0.88	1.40	2.13	3.23	7.63 ± 0.20
	12 h	0.98	1.35	2.06	3.19	7.58 ± 0.29
	24 h	0.96	1.90	1.67	2.58	7.10 ± 0.20
GlcNAc	4 h	0.77	1.29	2.06	3.10	7.23 ± 0.33
	12 h	0.94	1.27	2.17	2.69	7.06 ± 0.33
	24 h	0.81	0.65	1.00	2.15	4.60 ± 0.21

Intercellular gap scores were consistently low in the NON and DW groups. The AC (pH 3) and NF (pH 3) group scores decreased over time. The AC (pH 6) and NC (pH 3) group scores decreased gradually over time. Although scores for the NF (pH 6) group decreased gradually over time, scores at the 4-h time point were higher compared to those of the other groups, and the scores at the 24-h time point were higher than that of the control groups. Scores for the NC (pH 6) group remained high over all measured periods. Scores in the GlcNAc group were high until the 12-h time point but decreased by the 24-h time point.

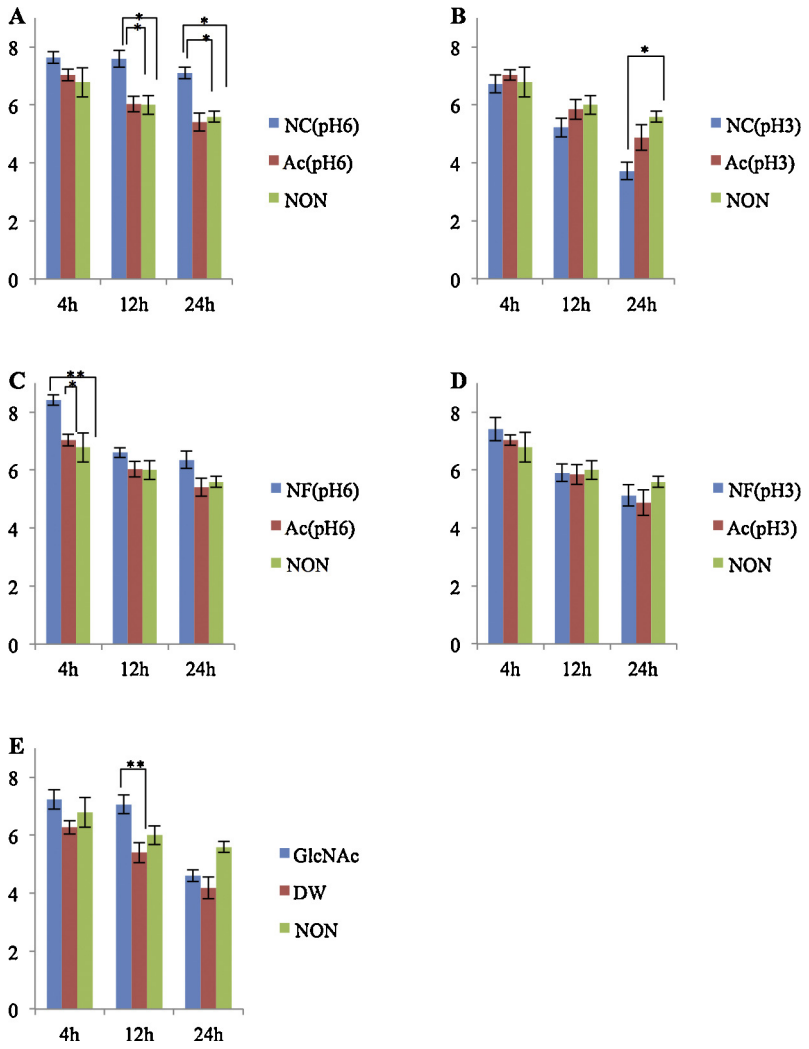

Fig. 2. Comparison of the results of histological scoring in each group. (*y*-axis, total scores; *x*-axis, incubation time). (A) Comparison of the NC (pH 6) group and the corresponding control groups, AC (pH 6) and NON. (B) Comparison of the NC (pH 3) group and the corresponding control groups, AC (pH 3) and NON. (C) Comparison of the NF (pH 6) group and the corresponding control groups, AC (pH 6) and NON. (D) Comparison of the NF (pH 3) group and the corresponding control groups, AC (pH 3) and NON. (E) Comparison of the GlcNAc group and the corresponding control groups, DW and NON. In the NC (pH 6) group, scores were significantly higher compared to those in the AC (pH 6) and NON groups 12 and 24 h post-application. In the NC (pH 3) group, scores were significantly higher compared to those in the NON group 24 h post-application. In the NF (pH 6) group, scores were significantly higher compared to those in AC (pH 6) and NON groups 4 h post-application. In the GlcNAc group, scores were significantly higher compared to those in the DW group 12 h post-application. The error bars indicate mean ± SE. Significantly different from the AC group ($^{**}p < 0.01$; $^{*}p < 0.05$).

cell concentrations score was maintained at 1.9 points 24 h post-application. However, the intercellular gap and nucleus clarity scores were relatively low (0.2–0.4 points and 0.3–0.4 points, respectively) 12 h post-application.

In the DW-treated group, the granular layer score was over 2.5 until 4 h post-application, after which time, it fell below 2.5 and was very low 24-h post-application, and the granule cell density and intercellular gap scores 24 h post-application were low (1.1 and 0.2 points, respectively).

In the AC (pH 3) group, the granular layer scores 12 h post-application were 2.5, and gradually decreased below 2.5 points by 24 h post-application. The granule cell density score was 1.3 points 12 h post-application and 1.1 points 24 h post-application.

In the Ac (pH 6) group, although the granular layer score was below 2.5 at 24 h post-application, scores for granule cell density (1.5 points), intercellular gap (0.7 point) and nucleus clarity (0.9 points) indicated good results.

In the NF (pH 3) group, the granular layer scores 4 h post-application were above 2.5; however, they subsequently decreased by 12 h post-application. Similarly, the granule cell density scores were high (1.9 points) 4 h post-application, but subsequently fell to 0.8–1.3 points by 12 h post-application. The intercellular gap and nucleus clarity scores were favorable 12 h post-application (1.3–1.6 and 1.0 points, respectively).

At all measured time points, the granular layer scores for the NF (pH 6) group were over 2.5, and the scores for granule cell density (1.7–2.5 points), intercellular gap (1.0–1.3 points), and nucleus clarity (0.9–1.0 points) were also maintained at satisfactory values post-application.

Granular layer scores for the NC (pH 3) group fell below 2.5 points beginning 12 h post-application. Granule cell scores were also low (0.5–1.2 points) after this time. Both the intercellular gap and nucleus clarity scores remained constant (1 point) at all the measured time points.

Similar to the NF (pH 6) group, the granular layer scores for the NC (pH 6) group were above 2.5 at all measured time points. Additionally, scores for granule cell concentrations (1.7–2.1 points), intercellular gap (1.4–1.9 points), and nucleus clarity (0.9–1.0 points) remained satisfactory post-application.

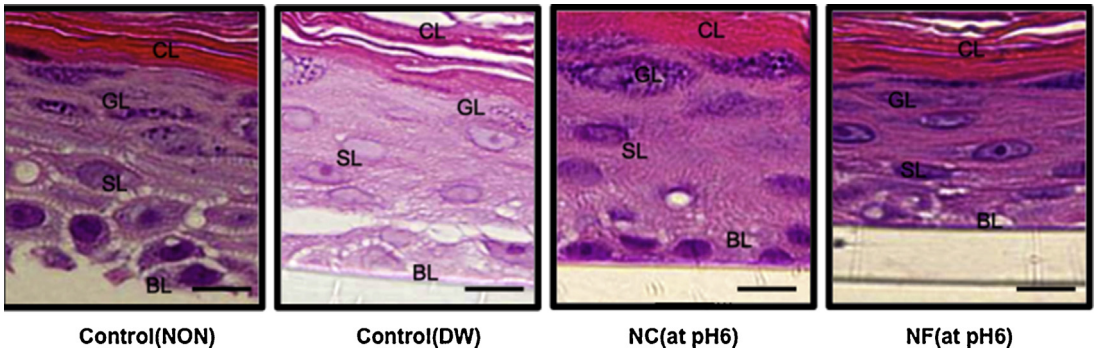

Fig. 3. The effect of chitin nanofibrils on the EPI-MODEL after 24 h of incubation. The number of layers and granule density were assessed in the granular layer (GL). Intercellular gaps and nucleus clarity were assessed in the spinosum layer (SL). Characteristic observations included large intercellular gaps in the NON group, low granule density in the DW group and high granule density in the NC (pH 6) and NF (pH 6) group. (bar = 100 μm).

In the GlcNAc group, all measured values were satisfactory until 12 h post-application; however, 24 h post-application, scores for the granular layer fell below 2.5, while granule cell density and intercellular gap scores were low, at 1.0 and 0.6 points, respectively.

Comparisons for each group are shown in Fig. 2. Furthermore, histological images for the NON, DW, NC (pH 6), and NF (pH 6) groups 24 h post-application are shown in Fig. 3.

At 12 and 24 h post-application, the NC (pH 6) group scores were significantly higher scores than those of the AC (pH 6) and NON groups ($p < 0.05$). In contrast, the NC (pH 3) group scores were significantly lower than that of the NON group 24 h post-application ($p < 0.05$). At 4 h post-application, scores for the NF (pH 6) group were significantly higher than those of the AC (pH 6) and NON groups ($p < 0.01$). The GlcNAc group scores were significantly higher 12 h post-application compared to those of the DW group ($p < 0.01$).

3.2. Experiment 2: effect of NF on skin cytokine production using Franz cells

The cumulative secreted cytokine concentration in the supernatant (PBS) from each experimental group is shown in Fig. 4.

For both IL-1α and TGF-β, the cytokine production increased in the following order: NF < NC < DW < AC. The TGF-β levels differed significantly between the NF and AC groups ($p < 0.01$), and the NC and AC groups ($p < 0.05$).

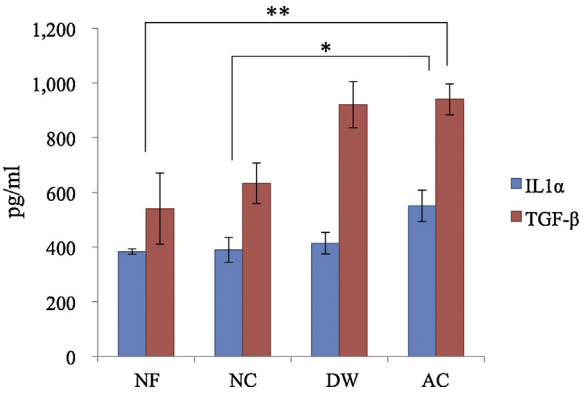

Fig. 4. Estimated production of cytokines in each group. For both IL-1α and TGF-β, the cumulative cytokine production increased in the following order: NF < NC < DW < AC. A highly significant difference was confirmed between the NF and DW groups (IL-1α and TGF-β) and the NF and AC groups (for TGF-β), whereas a significant difference was confirmed between the NC and AC groups (IL-1α and TGF-β). The error bars indicate mean ± SE. Significantly different from the AC group (**$p < 0.01$; *$p < 0.05$).

4. Discussion

4.1. Experiment 1: the effect of chitin NF on epithelial cells in a three-dimensional skin culture model

The skin, which is responsible for protecting various internal organs from the external environment, is composed of the epithelium and the corium and is supported by subcutaneous tissues. The epithelium consists of the cornified layer (CL), granular layer (GL), spinosum layer (SL), and basal layer (BL). Of the skin layers, the CL is responsible for acting as a protective barrier, and hence is an important part of the epithelium as it protects the internal structures from desiccation or against changes in the environment, while maintaining appropriate hydration for function within the environment, for example, UV, desiccation and chemical substances. (Rawlings & Harding, 2004). Secretions from the sebaceous glands that cover the outermost layer, secretions from granule cells, and keratinocytes participate in CL formation. Intercellular lipids and natural moisturizing factors (NMF) are composed of secretions from granule cells in the CL, and facilitate the barrier and moisturizing functions. NMFs are complex mixtures of lactic acid, urea, citrate, sugars, and amino acids such as pyrrolidone carboxylic acid (PCA), urocanic acid and its derivatives (Cler & Fourtanier, 1981). Intercellular lipids regulate moisture evaporation from the skin, but this phenomenon is known to decrease with age. In senile xerosis, a reduction in the number of keratohyalin granules has been observed (Tezuka, 1983), and there are reports that the granule cells and lamellar body numbers increase in hairless mice grown under dry environments (Denda et al., 1998). The essential role that NMFs play in the moisturizing and barrier functions of skin underscores the critical function of the granular layer and the associated granules, as they are responsible for secretion of both lipids and NMFs. Additionally, it has been reported that tight junctions in the second uppermost layer (SG2) of the granular layer seal intercellular gaps (Kubo, Nagao, Yokouchi, Sasaki, & Amagai, 2009).

Our current study reveals that even if topical treatments are not directly applied to the CL, the maintenance of proper culture and moisturizing conditions below the epithelium leads to favorable granular layer development, with an increase in granule density. However, if skin cells were cultured without the application of substances to the CL, low intercellular gap and nucleus clarity scores were obtained and maintenance of cellular integrity was not possible. Similar to previous studies, our current report suggests that the granule cell number is increased as a defense mechanism upon disruption of cellular integrity.

As shown in Fig. 2A and C, both the NF (pH 6) and NC (pH 6) group scores were favorable compared to those of their respective controls or the NON group, at all measured time points. Application

of NF (pH 6) or NC (pH 6) appears result in tighter intercellular spacing and promotes the maintenance of cellular integrity, when compared to non-treated cells.

These results suggest that the application of chitin NF to skin protects epithelial cells. Although the precise mechanism remains unknown, this effect may be attributable to its ability to prevent moisture evaporation. Moreover, as shown in Fig. 2A and B, the NC (pH 6) group scored higher on measured criteria compared to the NF (pH 6) group at all time points after the first 8 h of application, indicating that NC is the more effective skin protector in the long-term. In contrast, as shown in Fig. 2B and D, the scores for NF (pH 3) and NC (pH 3) decreased compared to those of the control or NON groups, beginning at 12 h post-application. This suggests that pH is an important criterion for topical formulations, and that pH 6 is more effective than pH 3 for epithelial cell protection.

In the GlcNAc group, the granular layer score fell below 2.5 points by 24 h post-application. At this time, the granule cell density and intercellular gap scores were 1.0 and 0.6 points, respectively. Histological Images 24 h post-application revealed a granular layer that had nearly disappeared or was 1-layer thick in some portions of the image. As stated above, granule cells secrete substances that constitute the CL, thereby conferring its barrier function. Furthermore, there are tight junctions in the SG2 layer of the granular layer, which in combination with the granule density and number of layers within the cell, are likely important for its barrier function. The granular layer score 24 h post-application for the GlcNAc group was 2.1 points, which is lower than that of the NF (pH 6) and NC (pH 6) groups. In addition, the granule density was lower in the GlcNAc group than the NF (pH 6) and NC (pH 6) groups. This suggests that the application of GlcNAc to the skin does not contribute to long-term skin cell protection. In contrast, 24 h post-application histological images of the NF- and NC-group samples showed that at least 2 layers of the granular layer were maintained and that many granules were present. All of these observations indicate that the application of NF (pH 6) and NC (pH 6) contributes more significantly to epithelial cell protection than does application of GlcNAc.

4.2. Experiment 2: effect of NF on skin cytokine production using Franz cells

Keratinocytes in skin produce a high level of IL-1α, and activated IL-1α is abundant in the cuticle (Kezic et al., 2012). Furthermore, molecules isolated from house dust mites have been shown to induce pro-inflammatory cytokine and chemokine release from epidermal keratinocytes and skin fibroblasts (Arlian & Morgan, 2011), there are many environmental stimuli that can be inflammatory. The cytokine TGF-β is secreted from T-cells and functions as an immunosuppressive factor. TGF-β regulates immune cell differentiation, proliferation, activation, and can contribute to pathologies such as cancer, autoimmunity, and opportunistic infection (Letterio & Roberts, 1998). TGF-β is a suppressive factor that regulates wound and skin-inflammation-related cellular processes (Anthoni et al., 2007).

In mouse hepatocytes, TGF-β suppresses the IL-1α-induced expression of IL-1R as well as TLR2 (Matsumura et al., 2004). Patients with osteomyelofibrosis have activated NF-κB due to monocyte adhesion, leading to IL-1 production, which in turn stimulates TGF-β production and causes bone marrow fibrosis (Rameshwar et al., 2000). Based on these interactions, inflammatory cytokines such as IL-1α and suppressive cytokines such as TGF-β are intimately related. Findings from a *Nocardia brasiliensis*-induced mouse footpad immunoreactivity model showed that both inflammatory- and anti-inflammatory cytokines are produced simultaneously by host cells (Solis-Soto et al., 2008). Taken together, the involvement of IL-1 in TGF-β production can be explained through a similar model, whereby production of TGF-β is intricately linked to the production of IL-1.

In our current study, the sum of cytokine concentrations at each time point was considered as the cumulative cytokine production level. The cumulative cytokine production level in the NF and NC groups was lower than that in the AC and DW groups. Although a significant difference in the IL-1 production in the NF/NC and AC/DW groups was not observed, a significant difference in TGF-β production was detected. TGF-β production in the NF (pH 6) group was lower than that in the NC (pH 6) group. On the other hand, the NC (pH 6) group scored was higher on measured criteria compared to the NF (pH 6) group in experiment 1. These experiments revealed that NF and NC protected skin cells. The reason of the difference in effects for skin protect between the two materials was still unclear. One of the mechanisms was considered that 3D structure of NF and NC contained water and prevent from skin dryness. In future, it needs further research to verify mechanisms of reduction of inflammatory cytokine when NF and NC were applied to skin.

5. Conclusions

The results of our study suggested that NF and NC protect skin cells while being less inflammatory. Further research is necessary to determine precisely how NF and NC can be incorporated into the manufacture of cosmetics or textiles.

Conflicts of interest

There is no conflict of interest.

Acknowledgment

This work was supported by a Tottori prefecture-financed aid project for beauty & health products (2011–2012).

References

Anthoni, M., Wang, G., Deng, C., Wolff, H. J., Lauerma, A. I., & Alenius, H. T. (2007). Smad3 signal transducer regulates skin inflammation and specific IgE response in murine model of atopic dermatitis. *Journal of Investigative Dermatology*, *127*, 1923–1929.

Arlian, L. G., & Morgan, M. S. (2011). Immunomodulation of skin cytokine secretion by house dust mite extracts. *International Archives of Allergy and Immunology*, *156*, 171–178.

Azuma, K., Osaki, T., Wakuda, T., Ifuku, S., Saimoto, H., Tsuka, T., et al. (2012). Beneficial and preventive effect of chitin nanofibrils in a dextran sulfate sodium-induced acute ulcerative colitis model. *Carbohydrate Polymers*, *87*, 1399–1403.

Chen, P. Y., Lin, A. Y., McKittrick, J., & Meyers, M. A. (2008). Structure and mechanical properties of crab exoskeletons. *Acta Biomaterialia*, *4*, 587–596.

Cler, E. J., & Fourtanier, A. (1981). L'acide pyrrolidone carboxylique (PCA) et la peau. *International Journal of Cosmetic Science*, *3*, 101–113.

Denda, M., Sato, J., Masuda, Y., Tsuchiya, T., Koyama, J., Kuramoto, M., et al. (1998). Exposure to a dry environment enhances epidermal permeability barrier function. *Journal of Investigative Dermatology*, *111*, 858–863.

Fabritius, H. O., Karsten, E. S., Balasundaram, K., Hild, S., Huemer, K., & Raabe, D. (2012). Correlation of structure, composition and local mechanical properties in the dorsal carapace of the edible crab Cancer pagurus. *Zeitschrift fur Kristallographie*, *227*(11), 766–776, 10.1524/zkri.2012.1532.

Fan, Y., Saito, T., & Isogai, A. (2008). Preparation of chitin nanofibers from squid pen beta-chitin by simple mechanical treatment under acid conditions. *Biomacromolecules*, *9*, 1919–1923.

Gopalan, N. K., & Dufresne, A. (2003). Crab shell chitin whisker reinforced 318 natural rubber nanocomposites 1. Processing and swelling behavior. *Biomacromolecules*, *4*, 657–665.

Ifuku, S., Nogi, M., Yoshioka, M., Morimoto, M., Yano, H., & Saimoto, H. (2010). Fibrillation of dried chitin into 10-20 nm nanofibers by a simple grinding method under acidic conditions. *Carbohydrate Polymers*, *81*, 134–139.

Ifuku, S., & Saimoto, H. (2012). Chitin nanofibers: Preparations, modifications, and applications. *Nanoscale*, *4*, 3308–3318.

Kezic, S., O'Regan, G. M., Lutter, R., Jakasa, I., Koster, E. S., Saunders, S., et al. (2012). Filaggrin loss-of-function mutations are associated with enhanced expression of IL-1 cytokines in the stratum corneum of patients with atopic dermatitis and in a

murine model of filaggrin deficiency. *Journal of Allergy and Clinical Immunology*, *4*, 1031–1039.
Kubo, A., Nagao, K., Yokouchi, M., Sasaki, H., & Amagai, M. (2009). External antigen uptake by Langerhans cells with reorganization of epidermal tight junction barriers. *Journal of Experimental Medicine*, *13*, 2937–2946.
Letterio, J. J., & Roberts, A. B. (1998). Regulation of immune responses by TGFβ. *Annual Review of Immunology*, *16*, 137–161.
Matsumura, T., Hayashi, H., Takii, T., Thorn, C. F., Whitehead, W. S., Inoue, J. I., et al. (2004). TGF-β down-regulates IL-1α induced TLR2 expression in murine hepatocytes. *Journal of Leukocyte Biology*, *75*, 1056–1061.
Minami, S. & Okamoto, Y. (2010). Tottori University, Drug for the treatment of the wound, Japan patent, 4,496,375. April 23.
Muzzarelli, R. A. A. (2009). Chitins and chitosans for the repair of wounded skin, nerve, cartilage and bone. *Carbohydrate Polymers*, *76*, 167–182.
Muzzarelli, R. A. A. (2010). Chitins and chitosans as immunoadjuvants and non-allergenic drug carriers. *Marine Drugs*, *8*, 292–312.
Muzzarelli, R. A. A., Morganti, P., Morganti, G., Palombo, P., Palombo, M., Biagini, G., et al. (2007). Chitin nanofibrils/chitosan glycolate composites as wound medicaments. *Carbohydrate Polymers*, *70*, 274–284.
Nikolov, S., Fabritius, H., Petrov, M., Friak, M., Lymperakis, L., Sachs, C., et al. (2011). Robustness and optimal use of design principles of arthropod exoskeletons studied by ab initio based multiscale simulations. *Journal of The Mechanical Behavior of Biomedical Materials*, *4*, 129–145.
Raabe, D., Romano, P., Sachs, C., Fabritius, H., Sawalmih, A. A., Yi, S. B., et al. (2006). Microstructure and crystallographic texture of the chitin–protein network in the biological composite material of the exoskeleton of the lobster *Homarus americanus*. *Materials Science and Engineering A*, *421*, 143–153.
Rameshwar, P., Narayanan, R., Qian, J., Denny, T. N., Colon, C., & Gasco′n, P. (2000). NF-kB as a central mediator in the induction of TGF-b in monocytes from patients with idiopathic myelofibrosis: An inflammatory response beyond the realm of homeostasis. *Journal of Immunology*, *165*, 2271–2277.
Rawlings, A. W., & Harding, C. R. (2004). Moisturization and skin barrier function. *Dermatologic Therapy*, *17*, 43–48.
Revol, J. F., & Marchessault, R. H. (1993). In vitro chiral nematic ordering of chitin crystallites. *International Journal of Biological Macromolecules*, *15*, 329–335.
Solis-Soto, J. M., Quintanilla-Rodriguez, L. E., Meester, I., Segoviano-Ramirez, J. C., Vazquez-Juarez, J. L., & Salinas Carmona, M. C. (2008). In situ detection and distribution of inflammatory cytokines during the course of infection with Nocardia brasiliensis. *Histology and Histopathology*, *23*, 573–581.
Tezuka, T. (1983). Electron-microscopic changes in xerosis senilis epidermis. Its abnormal membrane-coating formation. *Dermatologica*, *166*, 57–61.